

# Concepts and Measurement of Velocities and Viscosities at the Slag-Metal Interface

Luckman Muhmood\*<sup>1</sup> Nurni N Viswanathan<sup>2</sup> and Seshadri Seetharaman<sup>3</sup>

<sup>1</sup>CSIRO, Process Science and Engineering, Australia

<sup>2</sup>Professor, Luleå Technical University, Sweden

<sup>3</sup>Professor, Royal Institute of Technology, Sweden

**Abstract:** Dynamic studies on the mass transfer of surface-active elements from gas to molten iron through a suitable slag phase were carried out using sessile drop technique incorporating an x-ray imaging system. The surface active elements in focus were sulfur and oxygen using the slag systems CaO-SiO<sub>2</sub>-Al<sub>2</sub>O<sub>3</sub>-FeO and CaO-SiO<sub>2</sub>-Al<sub>2</sub>O<sub>3</sub> respectively. In both cases, the slag was saturated with alumina in order to prevent any slag compositional changes due to reactions with the alumina crucible. Proper sulfur and oxygen potentials were maintained in all phases for both cases. X-ray videos were taken that were later processed to identify the oscillation of the molten iron drop occurring during the mass transfer. The oscillations were traced to the surface movement occurring due to the concentration difference of sulfur/oxygen at the interface, which created an instantaneous area change at the slag-metal interface. This area change was due to the combined effect of Marangoni flow and interface dilatation. The velocities of sulfur and oxygen at the interface were calculated from the area change. The interfacial velocities had a maximum order of magnitude of 10<sup>-4</sup> m/s.

The change in area measured from the oscillations was attributed to the change in interfacial tension. The Interfacial dilatational modulus was evaluated for slag-metal systems at 1823 K. The high values of the dilatational modulus (5–10 times that obtained for surfactant adsorption) was directly related to the higher change in apparent interfacial tension prevailing at the slag-metal interface. The variation in the dilatational modulus was due to the non-uniform distribution of surface active elements at the interface and also to the varying surface pressure. Further, cold-model experiments were designed and carried out in order to estimate the surface shear viscosity. A relationship was established to find the surface/interfacial shear viscosity from the Newton's law of viscosity. The order of magnitude of the interfacial shear viscosity at the slag-metal interface was estimated from the values obtained earlier for the interfacial velocity. The order of magnitude obtained for slag-metal systems was roughly 10–100 times that usually occurring in colloidal systems.

**Keywords:** Interfacial Tension, Sulfur, Oxygen, Sessile Drop, Interfacial Velocity, Interfacial Dilatational Modulus, Interfacial Shear Viscosity

## 1. Introduction

Interfacial properties play a significant role in processes like refining, foaming and flotation. During dynamic mass transfer measurements, the interfacial area and energy continuously change and this response is of extreme importance to quantify the mass transfer rate. In metallurgy, the dynamic measurements of the interface have been confined to the variation of surface tension and contact angles<sup>1-10</sup>. However there are other areas that need to be stressed upon viz interfacial area change, the velocity of species at the interface, interfacial viscosities (both shear and dilatational) and dynamic surface tension.

The current work takes inspiration from the earlier works wherein it was reported that during intense mass transfer between two phases, very low apparent interfacial tension resulted<sup>11-13</sup>. In these works, iron containing higher oxygen content was introduced into a slag-iron system which was already maintained at equilibrium at a lower oxygen level. A sharp drop in the interfacial tension was observed caused by the surface-active oxygen and consequently, was dependent on the oxygen content in the liquid iron. This difference later decreased but was stabilized at a lower interfacial tension. However, since the mass transfer involved a solid-solid interface, the question arises regarding the precision of the values obtained.

Another work along which the concept of the present paper revolves is that of Jakobsson et al.<sup>14</sup> In this work, mass transfer of sulfur from gaseous phase to a metal drop through an alumina-saturated CaO-SiO<sub>2</sub>-Al<sub>2</sub>O<sub>3</sub>-FeO slag to the metal sample (sulfurization process) was envisaged. In this work, the source of sulfur would be a gas. In this way, the errors involved by mixing and other similar phenomena were reduced. It was observed using an X-ray source that, under dynamic conditions, the drop shape changed due to the sulfur movement along the interface and into the bulk of the drop. The property “interfacial velocity” using sulfur was estimated by these authors semi-empirically. The experiments needed precision and the data analysis as well as modelling required refinement.

Interfacial viscosity is the most important property that needs to be evaluated especially when rheological properties are of importance. Among the two important components of interfacial viscosity, *viz.* shear and dilatational, the latter is more important as its magnitude is generally higher and it provides a complementary method to describe the surfactant adsorption quantitatively<sup>15</sup>. In metallurgy, Hara et al.<sup>16</sup> used the rotating disc method for measuring the viscosity at the surface. In this method a plate disc was rotated and the viscosities at different layers were obtained by raising the rotating disc towards the surface. Popel et al.<sup>17</sup> used the oscillating method to measure the surface viscosity of iron oxide containing melts by adding MgO in small amounts. The surface viscosity of the melt was measured as the difference of the viscosity at the surface with and without MgO addition. However, it is well-known that the surface characteristics are quite different from the nature of the liquid at a few nanometers depth. Since the plate disc has a definite plate thickness, such experiments are restricted to millimeters scales; hence the values obtained would not represent the true value at the surface.

The current paper addresses the concept and measurement of the interfacial velocity of sulfur and oxygen at the slag metal interface. It also calculates the interfacial dilatational modulus at the interface which is related to the interfacial dilatational viscosity. This property is a measure of the extent of dilatation of the interface and is an indirect measure of the dynamic surface tension. In the later portion of the paper some cold model measurements of surface shear viscosity is made. Since the body of interest is a 2D surface rather than a 3D bulk liquid, using the Newton’s law of viscosity, the surface shear viscosity was estimated.

## 2. Theory

In the present work, the effect of surface-active elements like sulfur and oxygen at the iron–slag interface is considered as a means to measure the interfacial velocity. The surface active element, delivered by a gas mixture maintained at the required potentials at the surface of a slag passes through the slag and eventually reaches the molten

metal drop. The detailed methodology and concept is mentioned elsewhere <sup>18</sup>.

### Gas–slag–metal equilibrium

Equilibrium conditions for the gas–slag–metal system were maintained at 1823 K and 1 bar pressure. The equilibrium is represented in Figure 1. The gas mixture entering the furnace, especially the crucible, undergoes an instantaneous redox reaction due to the high temperature, and the gas containing the surface-active species dissociates forming S<sub>2</sub> and O<sub>2</sub> gas (if SO<sub>2</sub> gas is used) or O<sub>2</sub> (if CO<sub>2</sub> is used). In the case of sulphur, since both S<sub>2</sub> and O<sub>2</sub> are surface active in nature, a stringent control on the oxygen potential should be maintained such that the oxygen potential in the gas, slag and metal phases are equal, thus, ensuring that only S<sub>2</sub> enters the slag phase and later the metal, *via* the slag–metal interface.

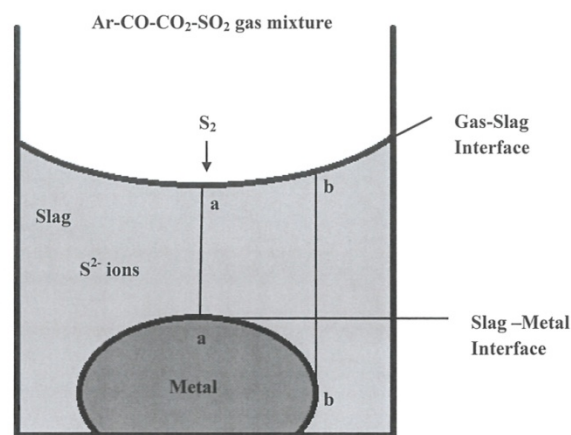
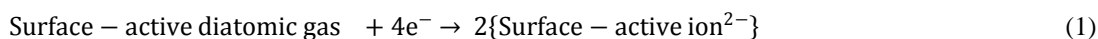
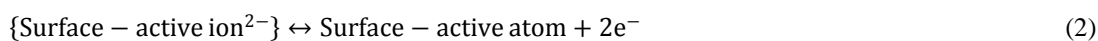


Figure 1: Gas-Slag-Metal equilibrium with interfaces. The distance ‘a-a’ between the gas-slag interface is smaller compared to ‘b-b’, hence sulfur reaches the slag metal interface at point ‘a’ prior to point ‘b’.

The surface active gas reaching the gas–slag interface then undergoes an electro-chemical reaction by which it forms corresponding ions:



These ions then move through the slag phase due to the chemical potential difference. Also, the forward movement of the surface-active ions is accompanied by a corresponding cation movement in order to maintain electrical neutrality. Thus the surface-active ions migrate to the slag–metal interface where they again undergo an electro-chemical reaction in which the ions are converted to atoms in the metal phase.



Owing to its surface-active behaviour, most of the atoms move along the surface of the metal drop while some of them enter the metal bulk phase up to a particular depth. Assuming that the electro-chemical reactions taking place at the interfaces are extremely fast <sup>19</sup> and the effect of the convection flow on mass transfer is negligible as the temperature gradient is insignificant, the surface velocity of the surface-active atom at the slag–metal interface can be estimated

from the oscillations produced due to its superficial movement. Further details are mentioned elsewhere<sup>18, 20</sup>.

### *Interface*

As seen earlier, interfacial velocity is the combined effect of the Marangoni force (force due to interfacial tension difference) and the forces that cause interface dilatation. Thus, it is of great interest to study the force balances at the interface during such a mass transfer process. The basic assumptions for the present approach are:

- i. Constant partial pressures of the surface-active species are maintained in the gas phase.
- ii. The interfacial reactions are electrochemical in nature and take place very fast in comparison with the diffusion process [8].
- iii. The diffusion of the surface-active atom into the bulk of the metal phase is much slower in comparison to the surface diffusion due to the availability of “dangling” metallic bonds at the interface.

The surface-active ion reaching the slag-metal interface will experience the following forces.

- a. An upward force towards the slag phase.
- b. A downward force towards the metal phase mainly due to the free metal bonds at the surface and due to the gravitational force, the latter in this case being negligible.
- c. A Marangoni force due to the surface/interface tension gradient on the surface of the metal drop at the slag-metal interface. The force acts along the interface in a direction towards the lower surface concentration of the surfactant.
- d. Dilatational force which causes an increase in the surface area due to the varying interfacial tension force.
- e. Brownian motion of the oxygen atoms which depends on the temperature of the system.

### *Dimension analysis and dependence on other properties*

In order to find a suitable equation for the interfacial velocity, dimension analysis approach was used. In this approach, the velocity is written as a function of the possible terms that would have a direct effect on it.

*Interfacial tension,  $\sigma$* : This variable has a direct effect on the interfacial velocity as it represents the degree of bonding at the surface. The greater the bonding, the lower will be the interfacial velocity. The surface tension can be measured from the contour of the sessile drop using the Adams-Bashforth equation<sup>21</sup>.

*Interfacial shear viscosity<sup>22</sup>,  $\mu_s$* : This variable has a limited impact on the interfacial velocity as it represents the resistance offered on the interfacial layer by the immediate layer beneath. It also depends on the interfacial tension, in the absence of an external shear force. It could be represented by the equation

$$\frac{\Delta\sigma}{\Delta R} = \mu_s \frac{\Delta v}{X}$$

*Interfacial dilatational viscosity<sup>23</sup>,  $K_d$* : It represents the increase in area due to the relative movement of the atom layers. It is represented as

$$\Delta\sigma = K_d \frac{1}{A_t} \frac{\Delta A}{\Delta t}$$

*Surface diffusion of sulfur in slag,  $D_s$* : This is related to the interfacial velocity as it directly represents the movement of the sulfur atoms due to concentration gradient at the interface. It is generally estimated by suitable chemical or tracer experiments.

Writing the surface velocity as a function of the above variables

$$v = f(\sigma, D_S, K_d, \mu_S) \quad (3)$$

Using the dimensional analysis approach

$$v = C \sigma^a D_S^b K_d^c \mu_S^d \quad (4)$$

Where 'C', 'a', 'b', 'c' and 'd' are constants.

By solving equation (4) in dimensional terms we get,

$$v = C \sqrt{\frac{\sigma D_S}{K_d}} \left[ \sqrt{\frac{D_S}{K_d \sigma}} \mu_S \right]^d \quad (5)$$

The term within the square brackets of equation (5) is dimensionless. Since C and d are constants that need to be calculated experimentally, an alternate way to solve equation (5) would be to collect the constants together to write the above equation as

$$v = \sqrt{\frac{\sigma D_S}{K_d}} \Phi \left[ \sqrt{\frac{D_S}{K_d \sigma}} \mu_S \right] \quad (6)$$

Where  $\Phi$  is a function given as

$$\Phi \left[ \sqrt{\frac{D_S}{K_d \sigma}} \mu_S \right] = C \left[ \sqrt{\frac{D_S}{K_d \sigma}} \mu_S \right]^d \quad (7)$$

It can be estimated by plotting the graph taking  $v \sqrt{\frac{K_d}{\sigma D_S}}$  on the y-axis and  $\mu_S \sqrt{\frac{D_S}{K_d \sigma}}$  on the x-axis. A smooth curve could be fitted to find the nature of the unknown function.

During dynamic studies, it is not reliable to calculate the interfacial tension since non-equilibrium conditions prevail. However the interfacial tension values can be substituted with contact angle as

$$\sigma = k'' / \cos\theta$$

Interfacial velocity can be measured for surface active elements like oxygen, sulfur and phosphorous all of which are important in metallurgy. Depending on the size of these atoms and the affinity of the free iron bonds on the metal surface to attract them, the interfacial velocities may vary. A higher velocity would indicate an easy removal from the surface during refining. Further, since there is a dilatational term involved, the interfacial area change would play a crucial role in the refining process as well.

### *Interfacial Velocity*

As discussed earlier, the movement of the surface-active species along the interface of the sessile drop could be traced by the fluctuations in the surface of the drop. In order to estimate the surface velocity due to the concentration variation along the interface, the oscillation of the drop should be taken into consideration. The oscillations of the drop would lead to a change in the surface area of the metal drop. This change in surface area could be equated with a circle

of a defined radius. Hence the change in the drop shape due to oscillation would lead to the change in surface area and consequently, change in radius of the circle. As both the cause and effect of the change in drop surface area could be attributed to the sulfur concentration change along the interface, one cycle consisting of a dip and rebound of the interface area are needed to be considered at a time.

If  $R_t$  is the radius of the equivalent circle of the drop with initial surface area  $A_t$  at any time  $t$  and  $R_{t+\Delta t}$  be the radius of the circle for drop with surface area  $A_{t+\Delta t}$  at the next instant  $t+\Delta t$ , the relationship between the change in interfacial velocity at the interface and the rate of change of the radius causing the oscillation of the drop is given by the equation

$$v_{\text{instantaneous}} = \frac{R_{t+\Delta t} - R_t}{\Delta t} \quad (8)$$

In case of the experiments where visualization could be envisaged in the direction perpendicular to the surface/interface, the direction and velocity (in such experiments tracer velocity) can be obtained in a straight-forward manner. However the velocity in these experiments would be dampened by the inertia force of the tracer particle or could be enhanced by the velocity of the gaseous medium.

#### *Interfacial Dilatational Modulus*

Surface active elements could be transferred from the gas phase to the metal phase *via* a slag phase as explained in the previous section. As the slag and metal were maintained at equilibrium by keeping the temperature constant throughout the experiment, the thermal convection in the slag and metal phases were assumed to be negligible. Hence diffusion through slag medium was the only possible mechanism for the surface active element to reach the slag-metal interface. It was also assumed that, since the electrochemical reactions taking place at the slag-metal interface were instantaneous, their effect could be neglected. An interfacial tension gradient along the slag-metal interface is created which would induce Marangoni flow leading to the flattening of the drop. The flow of the surface active element along the contour of the metal drop together with the diffusion of sulfur into the bulk would result in the depletion of sulfur from the top of the metal drop, which in turn, would regain its shape temporarily.

Once the dynamic oscillations of the interface are captured using a CCD camera, the video is split up into frames and random oscillation are identified based on the area change. The instantaneous area of sessile drop could be estimated from a MATLAB®<sup>24</sup> program. In this program, areas of both the left as well as right sections of the interfacial area of the drop were calculated by identifying the axis of symmetry.

The interfacial dilatational modulus, which is a measure of the interfacial resistance to changes in area, can be calculated from the equation<sup>15</sup>:

$$\epsilon = \frac{d\sigma}{d\ln A} \quad (9)$$

Where  $\epsilon$  the interfacial dilatational modulus in  $\text{mN}\cdot\text{m}^{-1}$  is,  $d\sigma$  is the change in interfacial tension from the equilibrium value and  $A$  is the interfacial area change from the equilibrium value. In the present calculations, the equilibrium value is taken as the equilibrium state prior to the injection of the surface active element source.

Another aspect is the calculation of the interfacial tension. The estimation of the interfacial tension from the sessile drop contour under dynamic mass transfer is very difficult due to the unstable sessile drop contour, the fact being that the stable condition of the drop is obtained from the force equilibrium between the gravitational force and the surface/interface tension force. A change in the interfacial tension could cause a sudden imbalance in the drop shape. The time lag for the drop to relax from this unsteady position is more than the frame speed at which the individual frames are obtained from the software.

Taking this into consideration, the apparent interfacial tension was estimated from the surface tensions of the individual phases with the same substrate, gaseous conditions and temperature. The interfacial tension could be calculated from the equation:

$$\sigma = \frac{\sigma_m \cos \theta_1 - \sigma_s \cos \theta_2}{\cos \theta} \quad (10)$$

Where,

$\sigma$  is the interfacial of the slag-metal interface with alumina substrate,  $\text{mN.m}^{-1}$ .

$\sigma_m$  is the surface tension of iron on alumina substrate,  $\text{mN.m}^{-1}$ .

$\sigma_s$  is the surface tension of slag on alumina substrate,  $\text{mN.m}^{-1}$ .

$\cos \theta_1$  is the contact angle of metal with alumina substrate .

$\cos \theta_2$  is the contact angle of slag with alumina substrate .

#### *Surface Shear Viscosity*

For this experiment, a suitable tracer was used for measuring the surface shear viscosity of the fluid. The tracer was chosen such that it neither has any solubility nor a tendency to absorption for the fluid. At the same time, the density of the tracer should be very less in comparison with the fluid density. Once the suitable tracer was chosen, it is kept on the stationary fluid surface maintained at any temperature T, K. Later the surface is tilted to a known degree of inclination and with the help of a CCD camera; the motion of the tracer is recorded. As seen from the figure, the shear force that causes the motion of the tracer is  $m.g.\sin \Theta$  and the thi  
the tracer in the fluid.

From Newton's law of viscosity the following relation can be written

$$\frac{mg \sin \theta}{A} = \mu_s \frac{v}{h} \quad (11)$$

Where,

m is the mass of the tracer used, kg

g is the acceleration due to gravity,  $\text{m.s}^{-2}$

$\Theta$  is the angle of inclination of the surface with the horizontal

A is the contact area,  $\text{m}^2$

$\mu_s$  is the surface shear viscosity, Pa.s

v is the velocity of the tracer,  $\text{m.s}^{-1}$

h is the immersion depth, m

The estimation of the immersion depth can be obtained from Archimedes principle, while the velocity of the tracer can be measured using a CCD camera.

Since it is the surface viscosity that is of interest and not the bulk, the surface would be considered as a 2D surface rather than a 3D solid. In such cases, the area term in the left hand side of equation should be substituted with the immersed perimeter of the tracer. Hence the unit of the surface shear viscosity, when perimeter is considered, is (N.m<sup>-1</sup>).s. This unit is similar to that of the surface viscosity terms often used in colloidal science. Hence it can be understood that keeping other factors constant, the smaller the tracer size, the more accurate is the experimental result as compared to the conventional results obtained using a monolayer surface or film. Hence equation (11) for surfaces can also be written as

$$\frac{mg\sin\theta}{P} = \mu_s \frac{v}{h} \quad (12)$$

Where, P is the perimeter of the immersed area.

### 3. Results and Discussion

#### *Interfacial Velocity of Sulfur and Oxygen*

After the X-ray video imaging, the initial step for the evaluation of the interfacial velocity was to identify the oscillations. This was done after converting the video to frames at the rate of 25 fps. The possible ways for oscillation identification was to plot the variation of surface tension with time or plot the variation of the contact angle with time. Since the estimation of the interfacial tension from the sessile drop contour under dynamic mass transfer is very difficult due to the unstable sessile drop contour, the contact angle was used as method to identify the oscillations.

Accordingly, the contact angles (both left and right) for the drop at 1823 K held for approximately 110 min was taken as the stable configuration. The sessile drop was analyzed for maximum height/width variations for identifying time zone for further analyses. Later frames from these time zones were analyzed for the deviation of the contact angles from the stable configuration. It could be identified that there were two modes of oscillations<sup>18, 20</sup>: one in which the left and right contact angles either both increased or decreased at the same time (which was called symmetric oscillations based on the concept put forward by Jakobsson et al.<sup>14</sup>) and the other where the increase/decrease of the left contact angle resulted in a decrease/increase of the right contact angle (these oscillations were termed as asymmetric oscillations). The reason for the asymmetric oscillations could be due to the deviation of the position of the sessile drop from the actual centre, slight inclination of the surface or uneven thermal expansion of the alumina shielding material. The variation in the contact angle ranged from 8°-16° which is well-acceptable. Oscillations were captured from the time the contact angles of the iron drop matched with that of the stable configuration. Figure 2 shows the two modes of oscillations taking place during dynamic mass transfer.



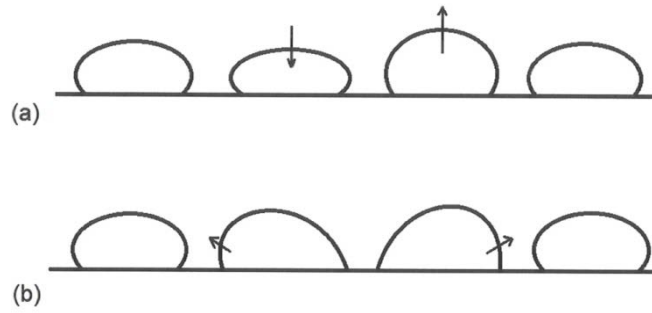


Figure 2: Modes of oscillation occurring during mass-transfer of sulfur (a) symmetric (b) asymmetric.

The oscillations were assumed to follow a sinusoidal curve and hence the total angular displacement due to the combination of symmetric and asymmetric parts can be written as

$$R = A_1 \sin(\omega_1 t) + A_2 \sin(\omega_2 t + \Theta) \quad (13)$$

Where  $A_1$  and  $A_2$  are the amplitudes of the symmetric and asymmetric oscillations respectively,  $\omega_1$  and  $\omega_2$  are the oscillation frequencies, and  $\Theta$  the phase difference between the oscillations

An effort was made to mathematically distinguish these oscillations; however, it was quite difficult to get a reasonable non-linear curve fit from the data points.

The angle variation from the stable configuration for the left contact angle as a function of time when sulfur was used as the surface active element is shown in Figure 3. It can be seen that the deviation from the stable profile of the drop increases with time but later tends to decrease as it reaches roughly 2222 s. This shows that the oscillations increase to a maximum amplitude roughly at 1016s. Further, it can be observed that the deviation from the stable profile tends to be positive as time increases indicating that the surface-active species has been absorbed by the drop and the contact angles have decreased resulting in a lower interfacial tension.

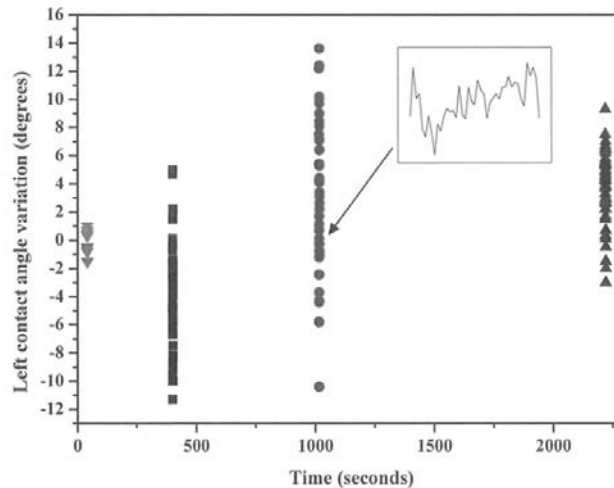


Figure 3: Variation of Left contact angle as a function of time when sulfur was used as surface active element. The time frames 39 -41, 399-402, 1016-1018 and 2220-2222 seconds are too small for the time scale hence the contact angle variation appears piled one over the other. Inset in the graph are the oscillations for time frame 1016-1018 seconds. The deviation of the left contact angles from the equilibrium value for time frame 39-41 seconds was shown in order to observe the oscillations occurring due to the sulfur concentration variation at the interface and not due to thermal convection.

After identifying individual oscillations three frames were taken for each oscillation which represent the first expansion (initial condition), depression (dip), and second expansion (rebound). These frames were then processed using a Didge image digitizing software. The software gave the coordinates of the contour of the sessile drop based on a scaling factor. This profile coordinates were later used to get the actual surface area of the sessile drop from a program written in MATLAB ®<sup>24</sup>. As mentioned before, the change in surface area between frames could be calculated and the interfacial velocity could be obtained. Figure 4 shows the variation in interfacial velocity as a function of time for both oxygen and sulfur used as surface active elements individually. The estimated error in measurement was  $\pm 6\%$ .

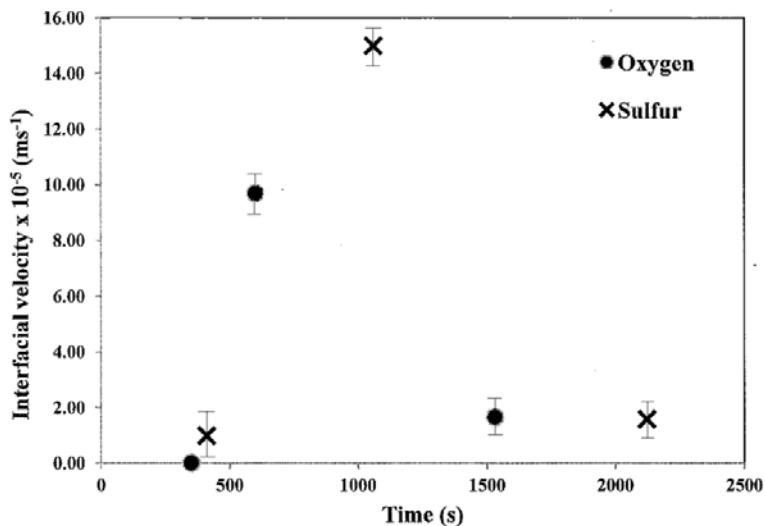


Figure 4: Comparison of interfacial velocities of oxygen and sulfur at 1823 K.

Similar experiments were also conducted at 1873 K in order to find out the effect of temperature on the interfacial velocity. Here the time frame was chosen corresponding to the maximum oscillation amplitude at 1823 K. The whole frame processing steps were repeated. Computation of the interfacial velocity at 1873 K shows that there is no significant change in the interfacial velocity of oxygen with temperature increase (Figure 5). However, in the case of sulfur a significant increase was observed (Figure 6). A comparison of the viscosity, interfacial velocity and interaction coefficient of the slag used for both sulfur and oxygen interfacial velocity measurements is shown in Table I.

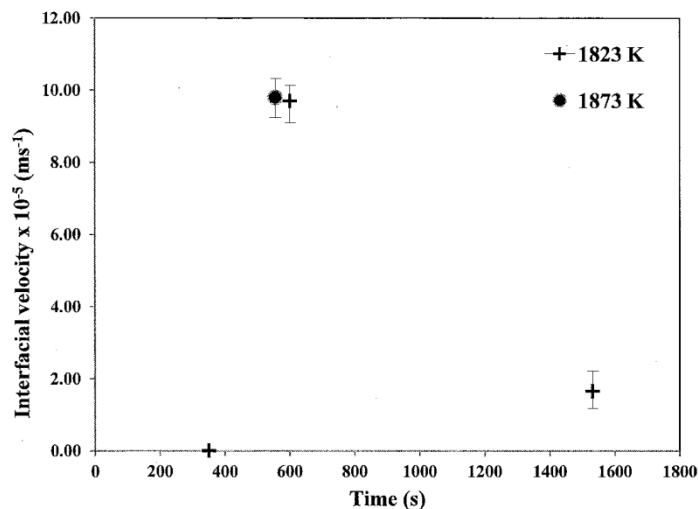


Figure 5: Interfacial velocity variation of oxygen as a function of time and temperature.

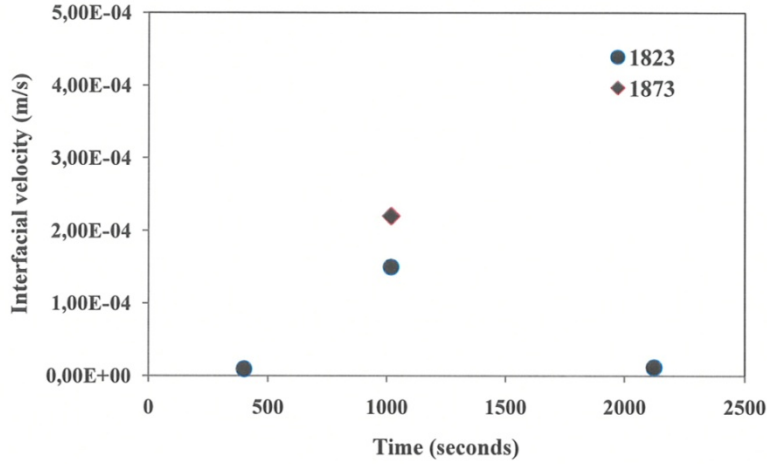


Figure 6: Interfacial velocity variation of sulfur as a function of time and temperature.

Table I: Viscosities, velocity and Interaction coefficients of slags used in sulfur and oxygen interfacial studies.

Slag Composition	Sulfur	Oxygen
CaO (wt%)	22.9	35
Al <sub>2</sub> O <sub>3</sub> (wt%)	54.1	55
SiO <sub>2</sub> (wt%)	18.0	10
FeO (wt%)	5	-
Atomic radius (pm) <sup>25</sup>	105±3	66±2
Interaction coefficient, $\phi$ at 1823 K	0.496	0.477
Interaction coefficient, $\phi$ at 1873 K	0.55	0.521
Viscosity, $\mu$ at 1823 K (poise) <sup>26,27</sup>	6.11	5.2 <sup>(a)</sup>
Viscosity, $\mu$ at 1873 K (poise) <sup>26,27</sup>	4.29	3.9
Maximum interfacial velocity at 1823 K (ms <sup>-1</sup> )	1.5 * 10 <sup>-4</sup>	9.7 * 10 <sup>-5</sup>
Maximum interfacial velocity at 1873 K (ms <sup>-1</sup> )	2.2 * 10 <sup>-4</sup>	9.8 * 10 <sup>-5</sup>

<sup>(a)</sup> CaO:Al<sub>2</sub>O<sub>3</sub>:SiO<sub>2</sub> ≡ 40:50:10

From Table I, it can be seen that the interaction coefficient for the slag used for oxygen studies is comparable to that used for sulfur studies. Although FeO addition to the slag reduces the viscosity, since the silica content of the slag used for sulfur experiments was almost twice that of the slag used for oxygen experiments, the viscosity for the CaO–Al<sub>2</sub>O<sub>3</sub>–SiO<sub>2</sub> slag was lower than that of the CaO–Al<sub>2</sub>O<sub>3</sub>–SiO<sub>2</sub>–FeO slag<sup>26,27</sup>. Both these characteristics point to the fact that the interfacial velocity of oxygen should be higher than that of sulfur. Also it can be observed that the atomic radius of sulfur is almost twice that of oxygen, hence the movement of sulfur across the interface is expected to be slower. However, the opposite actually occurs. The reason for this low interfacial velocity of oxygen is attributed to the high energy barrier (0.894 eV) at the free iron surface in comparison to sulfur (0.504 eV)<sup>28</sup>. It can also be observed from Figure 7 that the maximum velocity occurs faster in oxygen (620 s) in comparison to that of sulfur (1016 s). This shows that the diffusion of oxygen through slag is faster than that of sulfur.

#### Interfacial Dilatational Modulus

From the oscillations, the corresponding interfacial tension was measured using equation 10. Figure 7 shows the change in the interfacial tension as well as the interfacial dilatational modulus using sulfur as the surface-active element

for the left side and right side of the drop respectively. The value of the interfacial dilatation modulus for both the left and right sections of the interface was calculated using equation 9. The slag-metal interface at 1823 K was taken as the stable configuration. It can be seen that the values of the interfacial dilatational viscosity for slag-metal interfaces are roughly 5-10 times more than that observed in surfactant solutions dealt with in colloidal science. This is attributed essentially to the higher interfacial tension change at the slag-metal interface. A drastic change in interfacial tension especially around 1016 seconds from sulfur entry in the left portion of the slag-metal interface is observed which leads to higher interfacial dilatational viscosity.

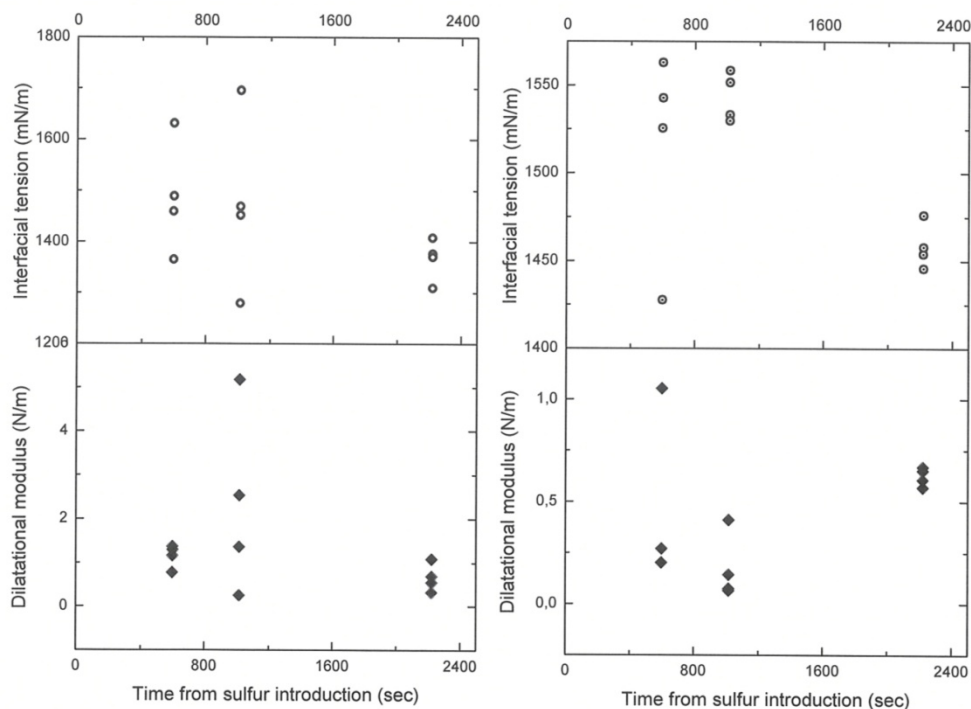


Figure 7: The variation of interfacial tension and dilatational modulus with time of introduction at the slag-metal interface using sulfur as the surface-active element for the left portion of the slag metal interface (left) and the right portion (right).

It is known that the interfacial dilatational viscosity is composition- as well as frequency-dependent<sup>29</sup>. Drastic changes in the dilatational viscosity show that sulfur is not uniform at the interface. Further atomistic investigations could throw light upon the preferential bonding between sulfur and the iron free surface. It can also be observed that the left and right portions of the slag-metal interface constitute different sulfur concentration regions which again can be verified by the interfacial tension difference. Another factor that could affect this change is the change in surface pressure. Since the drop does not have a flat surface, the pressure exerted on the surface would be less at the centre portion of the drop where the liquid slag height is less while the pressure would increase towards both ends. In colloids, the frequency of the dilatational modulus increases with increase of surface pressure<sup>29</sup>.

According to the definition of interfacial dilatational viscosity, this represents the resistance to the change in interfacial area. For a small time period, if there is a drastic difference in the dilatational viscosity, it could result in a sudden increase in area which consequently would lead to a higher interfacial velocity of the surface active species. From Figure 7, it can be seen that, by about 1016 seconds from sulfur entry into the slag-metal system, there is a drastic

change in interfacial dilatational viscosity, this in fact coincides with the maximum interfacial velocity of sulfur obtained earlier<sup>18</sup>.

Figure 8 shows the variation of interfacial tension as well as interfacial dilatational viscosity at 1823 K in the left and right side of the slag-metal interface when oxygen is used as a surface-active element. As it can be seen, the relationship between the two interfacial properties could clearly be observed. Similar variations could be observed for the interfacial dilatational viscosity in the left and right sections of the interface especially that for time 661 and 1550 seconds from the oxygen introduction into the metal-slag system. This explains the comparable order of magnitude of the interfacial velocity obtained earlier<sup>19</sup>.

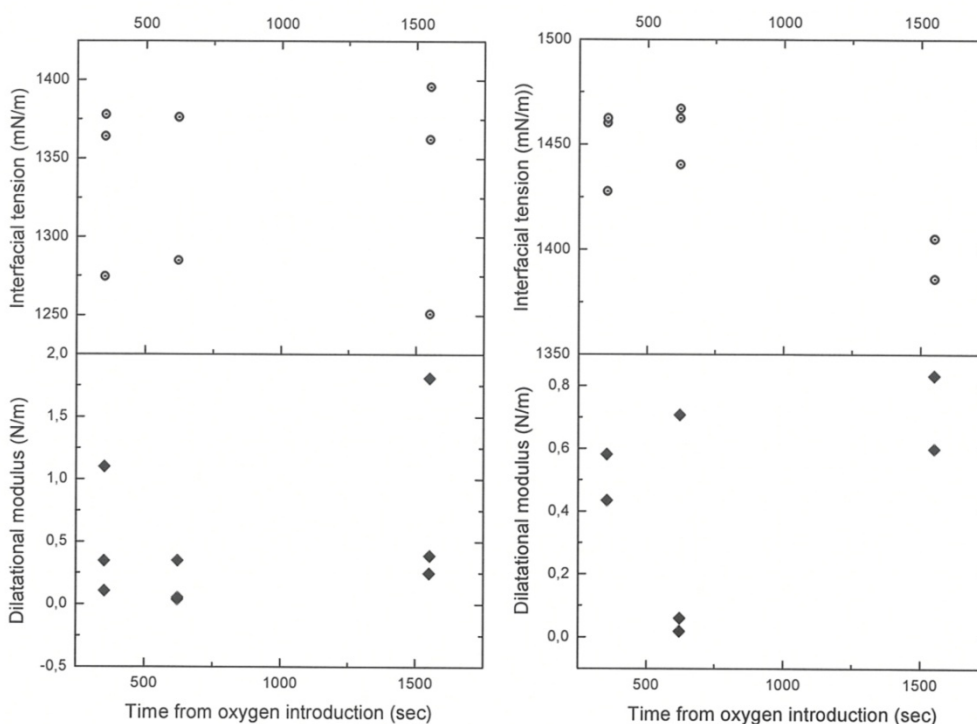


Figure 8: The variation of interfacial tension and dilatational modulus with time of introduction at the slag-metal interface using oxygen as the surface-active element for the left portion of the slag metal interface (left) and the right portion (right).

### Surface Shear Viscosity

The experimental methodology for the estimation of surface shear viscosity is mentioned elsewhere<sup>30</sup>. The aim of the whole exercise was to bring out a suitable technique for the measurement of interfacial/ surface shear viscosity in case of liquid metal, slag or slag-metal interface. The surface shear viscosity was measured at the air-water interface using thermocol as the tracer. Table II shows the results for the same tracer but at different temperatures. It can be seen that the experimental technique though not accurate enough can capture change in viscosity for slight temperatures.

Table II shows the surface viscosity results for different sizes of tracer used. Observing from the results, it could be seen that the experimental procedure showed more accuracy for the surface shear measurement when smaller size of tracer was used. Another surface viscosity experiment was made using a very small wooden splinter of dimensions 1.67

x 1 x 1 mm as the tracer. Since the experimental time was less, it could be assumed that the absorption of water by the splinter was very small. The results in Table III show that the experimental technique is consistent for similar sizes of tracers used.

Table II: Experimental results for different tracer sizes.

	Thermocol (radius=2.25x10 <sup>-3</sup> m)	Thermocol (radius=0.5 x10 <sup>-3</sup> m)
Immersion depth , h (m)	1.02 x 10 <sup>-3</sup>	2.58 x 10 <sup>-4</sup>
Surface velocity, v (m.s <sup>-1</sup> )	4.063 x 10 <sup>-4</sup>	6.5 x 10 <sup>-4</sup>
Inclination angle, $\Theta$ (degrees)	7.55	7.55
Shear Force (N)	8 x 10 <sup>-7</sup>	5.13 x 10 <sup>-8</sup>
Perimeter, P	6.406 x 10 <sup>-3</sup>	6.28 x 10 <sup>-4</sup>
Surface shear viscosity, $\mu_s$ (sP)	0.3135	0.03242

Table III: Experimental results with wooden splinter as tracer.

	Wood splinter
Immersion depth , h (m)	2.593 x 10 <sup>-4</sup>
Surface velocity, v (m.s <sup>-1</sup> )	2.855 x 10 <sup>-4</sup>
Inclination angle, $\Theta$ (degrees)	7.55
Shear Force (N)	1.289 x 10 <sup>-7</sup>
Perimeter, P	3.859 x 10 <sup>-3</sup>
Surface shear viscosity, $\mu_s$ (sP)	0.03034

As observed the methodology for the experiments was successful with respect to reproducibility for various tracer materials of similar sizes as well as to bring out the temperature dependence of surface viscosity. The absolute value for the shear viscosity at the surface would depend on the size of the tracer particle used. For liquid metal surfaces as well as slag-metal interfaces with a transparent slag surface, inclusions could be used as a suitable tracer material.

Assuming a circular inclusion of 1 $\mu$ m radius, the immersion depth would be of the same order. The average order of the interfacial velocity<sup>20</sup> is taken as 10<sup>-5</sup>m.s<sup>-1</sup> obtained from previous experiments. Using equation (7), the order of the interfacial shear viscosity would be roughly between 10<sup>-1</sup>-10<sup>-2</sup> mN.s .m<sup>-1</sup> (sP, also called surface poise)

An expression was earlier derived for the surface/interfacial velocity as shown in equation (5). So, the order of magnitude of the interfacial velocity would primarily depend on the order of magnitude of  $\sqrt{\frac{\sigma D_S}{K}}$ . The surface tension has the order 10<sup>-3</sup> N.m<sup>-1</sup> and the order of the dilatational viscosity (10<sup>-3</sup>(N.m<sup>-1</sup>).s) is similar to that of surface tension as seen in most of the colloidal systems<sup>15</sup>. The order of diffusivity is 10<sup>-10</sup> m<sup>2</sup>.s<sup>-1</sup>. Hence the order of magnitude of the interfacial velocity should be 10<sup>-5</sup>m.s<sup>-1</sup>. This value corresponds to the values obtained by earlier experiments<sup>18,20</sup>.

Looking at the values of C and d.

The order of magnitude of term given in square brackets

$D_S$  approximately 10<sup>-10</sup> m<sup>2</sup>.s<sup>-1</sup>

K approximately 10<sup>-3</sup>(N.m<sup>-1</sup>).s

$\sigma$  approximately 10<sup>-3</sup>(N.m<sup>-1</sup>)

$\mu_s$  Approximately 10<sup>-1</sup>-10<sup>-2</sup> sP (surface poise = (mN.m<sup>-1</sup>).s)

Hence d should be a fraction between 1/6 -1/7

C would be difficult to estimate as the exact values need to be known. Currently, for the CaO-SiO<sub>2</sub>-Al<sub>2</sub>O<sub>3</sub>-FeO molten slag-iron system, the values of the interfacial dilatational viscosity and the surface diffusion of sulfur in the slag for the particular slag-metal system are not precisely known. However the exact estimation of the constants 'C' and 'd' would depend on the slag-metal system used and also on the experimental temperature. By precise tracking of the oscillations, the experimentalist can achieve this feat.

#### 4. Summary

Some new observations occurring at the slag-metal interface during dynamic mass transfer has been addressed. The oscillations occurring at the interface due to the varying concentration of the surface active elements is of prime importance for estimating these properties. A suitable method was adopted to analyze these oscillations and to get the maximum information viz; interfacial velocity, interfacial dilatational modulus. A methodology was also put forward for estimating the interfacial shear viscosity. As these measurements and estimations are first of its kind, further implementation of sophisticated measurement techniques would be required for refining the results.

#### Acknowledgements

The authors would like to thank the Swedish Research Council (Project No: H 6971) for the financial support. Also L. Muhmood would like to thank CSIRO for the financial support to attend MOLTEEN 2012.

#### Nomenclature

- $\sigma$  The instantaneous interfacial tension difference from the equilibrium condition, mN.m<sup>-1</sup>  
 $\mu_s$  The interfacial shear viscosity, mN.m<sup>-1</sup>.s (sP)  
 $K_d$  The interfacial dilatational viscosity, mN.m<sup>-1</sup>.s (sP)  
 $v$  The surface/interfacial velocity, m.s<sup>-1</sup>  
 $X$  The thickness of the surface/Interface layer, m  
 $t$  Time, s  
 $A_t$  The instantaneous interfacial area at any time t, m<sup>2</sup>  
 $R$  The radius of the circle with area equivalent to the interfacial surface area, m  
 $D_s$  The surface diffusion of sulfur in slag, m<sup>2</sup>.s<sup>-1</sup>  
 $k''$  The apparent interfacial tension, mN.m<sup>-1</sup>  
 $T$  Temperature, K  
 $T_M$  The melting point of pure iron, K  
 $W_{ad}$  The work of adhesion between slag and metal, mN.m<sup>-1</sup>  
 $\sigma_m$  The surface tension of the metal at temperature T, K  
 $\sigma_s$  The surface tension of the slag at temperature T, K  
 $\sigma_{ms}$  The interfacial tension at the slag-metal interface at temperature T, K  
 $\emptyset$  The interaction coefficient  
 $W_{co}^m$  The work of cohesion of the metal phase, mN.m<sup>-1</sup>  
 $W_{co}^s$  The work of cohesion of the slag phase, mN.m<sup>-1</sup>  
 $\theta$  The contact angle, degrees  
 $R''$  The total angular displacement, radians  
 $A'$  The amplitudes of the oscillations

- $\omega$  The oscillation frequencies,  $s^{-1}$
- $\Theta$  The phase difference between the symmetric and asymmetric oscillations, degrees
- $\epsilon$  The Interfacial dilatational modulus,  $Nm^{-1}$

## References

- [1] G.R. Belton. *Met. and Mat. Trans. B*, 1976, 7B, p. 35-42.
- [2] K. Ogino, K. Nogi and C. Hosoi. *Tetsu-to-Hagané*, 1983, 69 (16), p. 1989-1994.
- [3] M. Divakar, J.P. Hajra, A. Jakobsson and S. Seetharaman. *Met. and Mat. Trans. B*, 2000, 31B, p. 267-276.
- [4] E. Kapilashrami, A.K. Lahiri, A.W. Cramb and S. Seetharaman. *Met. and Mat. Trans. B*, 2003, 34B, p. 647-652.
- [5] B.J. Keene, K.C. Mills, J.W. Bryant and E.D. Hondros. *Canadian Metallurgical Quarterly*, 1982, 21(4), p. 393-403.
- [6] Y. Chung and A.W. Cramb. *Met. and Mat. Trans. B*, 2000, 31B, p. 957-971.
- [7] H. Gaye, L.D. Lucas, M. Olette and P.V. Riboud. *Canadian Metallurgical Quarterly*, 1984, 23(2), p. 179-191.
- [8] A. Jakobsson, M. Nasu, J. Mangwiru, K.C. Mills and S. Seetharaman. *Phil. Trans. R. Soc. Lond. A*, 1998, 356, p. 995-1001.
- [9] P.V. Riboud and L.D. Lucas. *Canadian Metallurgical Quarterly*, 1981, 20(2), p. 199-208.
- [10] I. Jimbo and A.W. Cramb. *ISIJ International*, 1992, 32(1), p. 26-35.
- [11] Yu.A. Minaev and V.A. Grigorian. *Zavod. Lab.*, 1965, 31, p.809.
- [12] A.A. Deryabin, S.I. Popel and L.N. Saburov. *Izv. Akad. Nauk SSSR, Metallurgy*, 1968, 5, p.51.
- [13] K. Ogino, S. Hara, T. Miwa and S. Kimoto. *Trans. Iron and Steel Inst. Japan*, 1984, 24, p. 522-531.
- [14] A. Jakobsson, N.N. Vishwanathan, S. Du and S. Seetharaman. *Met. and Mat. Trans. B*, 2000, 31B, p. 973-980.
- [15] Y. Huang, Lei Zhang, Lu Zhang, L. Luo, S. Zhao and J. Yu. *J. Phys. Chem. B*, 111, 2007, p. 5640-5647.
- [16] S. Hara, M. Kitamura and K. Ogino. *ISIJ International*, 30 (9), 1990, p.714-721.
- [17] S.I. Popel, V.I. Sokolov and V.G. Korpachev. *Fiz. Khimii, Met. Rasplavov*, 1959, p. 24.
- [18] L. Muhmood, N. N Viswanathan, S Seetharaman . *Met. and Mat. Trans. B*, Vol 42(3), 2011, p. 460-470.
- [19] F.D. Richardson: *Physical Chemistry of Melts in Metallurgy*, Vol.2, Academic press, 1974.
- [20] L. Muhmood, N. N Viswanathan, S Seetharaman . *Int. J. Mat. Res.*, 2012, Accepted.
- [21] F. Bashforth and J.C. Adams: *An attempt to test the theories of capillarity*, Cambridge University Press, Cambridge, 1883.
- [22] A.W. Adamson: *Physical Chemistry of Surfaces*, 3<sup>rd</sup> edition, 1976, p.118.
- [23] F. van Voorst Vader, Th.F. Erkens and M. van den Temple. *Trans. Faraday Soc.*, 1964, 60, p. 1170.
- [24] MATLAB®: Mathworks®, ver. R2009b, 2009. <http://www.mathworks.com/>
- [25] J.F. Shackelford, W. Alexander (Ed.): *Materials Science and Engineering Handbook*, CRC Press, 3<sup>rd</sup> Edition, 2001, p. 22.
- [26] Thermoslag®: Division of Materials Process Science, Royal Institute of Technology, Stockholm, 1996.
- [27] P. Kozakevitch. *Rev. Métall.* 57(2), 1960 149.
- [28] W. Cao, A. Delin, S. Seetharaman. *Steel Res. Int.*, 81 (11), 2010, p. 949-952.
- [29] J. Lucassen and D. Giles. *J. Chem. Soc. Faraday Trans. 1*, 71, 1975, pp. 217-232.
- [30] L. Muhmood. *Steel Res. Int.*, vol. 82 (12), 2011, p. 1375-1384.